

~~CONFIDENTIAL~~

Copy 6  
RM E53J28

NACA RM E53J28



# RESEARCH MEMORANDUM

PRELIMINARY INVESTIGATION OF PERFORMANCE OF  
VARIABLE-THROAT EXTENDED-PLUG-TYPE NOZZLES  
OVER WIDE RANGE OF NOZZLE PRESSURE RATIOS

By Carl C. Ciepluch, H. George Krull, and Fred W. Steffen

Lewis Flight Propulsion Laboratory

Cleveland, Ohio  
CLASSIFICATION CHANGED

To: UNCLASSIFIED

By authority of NACA Research effective  
RA-121 Date Oct 14, 1957  
Amr 11-15-57

CLASSIFIED DOCUMENT

This material contains information affecting the National Defense of the United States within the meaning of the espionage laws, Title 18, U.S.C., Secs. 793 and 794, the transmission or revelation of which in any manner to an unauthorized person is prohibited by law.

NATIONAL ADVISORY COMMITTEE  
FOR AERONAUTICS

WASHINGTON

February 5, 1954

LIBRARY COPY  
FEB 10 1954  
LANGLEY AERONAUTICAL LABORATORY  
LIBRARY, NACA  
LANGLEY FIELD, VIRGINIA

~~CONFIDENTIAL~~



## NATIONAL ADVISORY COMMITTEE FOR AERONAUTICS

RESEARCH MEMORANDUM

## PRELIMINARY INVESTIGATION OF PERFORMANCE OF VARIABLE-THROAT

## EXTENDED-PLUG-TYPE NOZZLES OVER WIDE RANGE

## OF NOZZLE PRESSURE RATIOS

By Carl C. Ciepluch, H. George Krull, and Fred W. Steffen

## SUMMARY

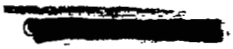
As part of an over-all program for the experimental investigation of large-scale jet nozzles, a preliminary evaluation of the internal performance characteristics of several variable-throat extended-plug-type nozzles was obtained over a range of nozzle pressure ratios from 1.5 to 15 with nozzle throat-area variations as great as 2:1.

An extended-plug nozzle attained peak thrust coefficients as high as those which have been attained with fixed-geometry convergent-divergent nozzles. The thrust coefficients of the extended-plug nozzles were relatively insensitive to both nozzle pressure ratio and throat area over the range investigated. The lack of sensitivity of thrust coefficient to nozzle pressure ratio and throat area was evidenced primarily by the absence of severe decreases in thrust coefficient at low nozzle pressure ratios which are normally observed for convergent-divergent nozzles because of overexpansion. For choked flow, the flow coefficients of the extended-plug nozzles varied from 0.95 to 0.997.

A ratio of the outer-shell exit area to nozzle throat area was found to be an important variable affecting nozzle performance. Most of the configurations reported herein showed a small decrease in thrust coefficient at low nozzle pressure ratios; however, it is believed that this characteristic can be nearly eliminated by proper nozzle design.

## INTRODUCTION

It is shown in references 1 to 3 that a convergent-divergent exhaust nozzle is needed for supersonic flight with a turbojet or ram-jet engine. In general, both the throat area and the expansion ratio of the convergent-divergent nozzle must be variable to provide for large changes in engine operating conditions. Several types of designs which may satisfy these requirements have been investigated.



The performance of one type of design, variable-throat convergent-divergent nozzle, with a fixed exit is reported in reference 4. These nozzles consisted of either a movable convergent-divergent conical-outer-shell and a fixed center plug or a series of fixed and movable vanes which formed convergent-divergent two-dimensional flow channels. Although variation in throat area was provided with these nozzles, the expansion ratio resulting from any throat area called for did not necessarily provide optimum expansion for the nozzle pressure ratio under a given condition of operation and, therefore, losses due to either under-expansion or overexpansion could result.

Another type of design which may provide more appropriate expansion ratios in some applications is the variable-throat extended-plug-type nozzle. A preliminary investigation of the extended-plug nozzle was conducted and the results obtained are reported herein. This nozzle consisted of a convergent conical outer shell and a conical plug. The nozzle throat area could be varied either by translating the conical outer shell along the plug or by using outer shells having various exit diameters at a fixed position on the plug to simulate an iris-type outer shell. In these nozzles, the external portion of the plug serves the same purpose as diverging walls of a conventional convergent-divergent nozzle; that is, it provides a surface on which the high pressure of the expanding jet can act.

The purpose of this investigation was to determine the magnitude of thrust coefficients that might be expected from several extended-plug nozzles over a range of nozzle pressure ratios and throat-area settings and to determine the effect of the important geometrical design variables on performance. The data obtained do not necessarily represent the optimum for this type of nozzle, because no attempt was made to refine the nozzle design; therefore, the data are not intended as final design criteria.

Three conical outer shells covering a range of nozzle exit areas and nozzle throat areas were used with a simple center plug. Provisions also were made to translate the outer shells along the plug so that the nozzle throat area could be varied. Each configuration was investigated over a range of nozzle pressure ratios from 1.5 to about 15.

## APPARATUS AND INSTRUMENTATION

### Installation

The nozzles were installed in a test chamber connected to the laboratory combustion air and the altitude exhaust facilities as shown in figures 1 and 2. The nozzles were mounted on a section of pipe which was freely supported on flexure plates shown in figure 2. The mounting

pipe was connected through a bell crank to a calibrated balanced-air-pressure diaphragm which was used in measuring thrust. A labyrinth seal around the necked-down inlet section ahead of the mounting pipe separated the nozzle-inlet air from the exhaust and provided a means of maintaining a pressure difference across the nozzle.

### Nozzle Configurations

The 10 nozzle configurations investigated are listed in table I along with their respective component parts. An exploded assembly of a typical configuration is shown in figure 3. The component parts of each configuration consisted of a spool piece, an outer shell, and a plug. The dimensions of the various parts used to make up the configurations are shown in figure 4. For the simulated translatable-outer-shell type nozzle (configurations A to F), nozzle-throat-area was varied by changing the position of the conical outer shell on the plug by means of the spool pieces. For the simulated iris-type nozzle (configurations B, G, and H), outer shells with exit diameters of 8.5, 10.5, and 13 inches were used to vary the nozzle throat area. Two plugs were investigated; plug 1 had a conical downstream section, while plug 2 had a blunt downstream end (see fig. 4(c)).

The flow-area variation along the plug for the translatable-outer-shell nozzle (configurations A to F) is shown in figure 5(a), and the variation in flow area along the plug for the simulated iris-type nozzle (configurations B, G, and H) is shown in figure 5(b). The internal flow area, represented by the solid lines, is the annular area between the plug and outer shell in a plane perpendicular to the axis of the plug. The diameter of the jet was assumed to be equal to the diameter of the outer-shell exit; therefore, the external flow area along the plug, as shown by the dashed curve, was equal to the annular area enclosed by the surfaces of the plug and a cylinder with a diameter equal to that of the outer-shell exit. These configurations covered a range of throat areas from about 43 to 89 square inches. From figure 5, it can also be seen that configurations B, C, D, E, and H had some internal divergence, which is listed in table I.

### Instrumentation

Pressures and temperatures were measured at various stations as shown in figure 2. At the air-flow measuring station (station 2) there were seven total-pressure probes, seven static-pressure probes, and three wall-static taps. At station 3, the nozzle inlet, the instrumentation consisted of 14 total-pressure probes and 6 thermocouples. Ambient-exhaust-pressure instrumentation was provided at station 0, and a static-pressure survey was made on the outside wall of the

mounting-pipe diffuser. The instrumentation on plug 1 consisted of 11 wall-static taps on the downstream conical section of the plug and 3 wall-static taps on the cylindrical section.

### PROCEDURE

Performance data for each configuration were obtained over a range of nozzle pressure ratios at a constant air flow. The nozzle pressure ratio was varied from about 1.5 to the maximum obtainable, which varied from configuration to configuration because of varying throat areas and limiting air-handling capacity of the air-supply and exhaust equipment.

The thrust coefficient was calculated by dividing the actual jet thrust by the ideal thrust. The actual jet thrust was obtained from the balanced-air-pressure-diaphragm measurements, and pressure and temperature measurements made throughout the test setup. The ideal jet thrust was calculated as the product of the measured mass flow and the isentropic jet velocity based on the nozzle pressure ratio and the inlet temperature. The symbols used in this report and the methods of calculation are shown in appendixes A and B, respectively.

### RESULTS AND DISCUSSION

#### General Performance Characteristics

The performance of a typical extended-plug nozzle over a range of nozzle pressure ratios is compared with the performance of a convergent nozzle and a fixed-geometry convergent-divergent nozzle in figure 6. The data for the convergent and convergent-divergent nozzles were taken from reference 1. Configuration D of the extended-plug nozzles and a convergent-divergent nozzle with an expansion ratio of 2.65 were chosen for comparison because both have thrust coefficients of approximately the same magnitude at a nozzle pressure ratio of 16, which is close to the design nozzle pressure ratio of the convergent-divergent nozzle. Configuration D and the convergent-divergent nozzle both have thrust coefficients of approximately 0.95 at a nozzle pressure ratio of 16, while the convergent nozzle, which is severely underexpanded, has a thrust coefficient of 0.89. In the extended-plug nozzle, the external plug surface takes the place of the divergent walls of a convergent-divergent nozzle as the surface on which the expanding jet acts; thus, higher thrust coefficients are reached at high pressure ratios with the extended-plug nozzle than with a simple convergent nozzle. At a nozzle pressure ratio of 2, the thrust coefficient of the extended-plug nozzle was 0.935 compared with values of 0.82 for the convergent-divergent nozzle and 0.98 for the convergent nozzle. The extended-plug nozzle not only has thrust coefficients equal to those of a convergent-divergent

nozzle at high nozzle pressure ratios, but it also has thrust coefficients approaching those of the convergent nozzle at low nozzle pressure ratios. The thrust coefficient of the extended-plug nozzle exceeds that of the convergent-divergent nozzle at lower nozzle pressure ratios because of less severe over-expansion losses.

3071 Performance of translatable-outer-shell type extended-plug nozzle. -  
Experimental thrust coefficients obtained over a range of nozzle pressure ratios are shown in figure 7 for configurations A to F (the configurations correspond to a nozzle with a fixed center plug and a translatable-outer-shell as the means of varying the nozzle throat area). The variation in relative throat area  $A_r$  (ratio of nozzle throat area to minimum nozzle throat area) was approximately 2:1. Configuration A approximated a convergent nozzle ( $A_g/A_t = 1$ ) and had a peak thrust coefficient of 0.97 which is slightly lower than that of the simple conical nozzle reported in reference 1. The difference in thrust coefficient was a result of the extended-plug nozzle having a larger internal wetted area which increased the skin friction. Maximum thrust coefficients of 0.96, 0.95, 0.95, 0.945, and 0.922 were obtained with configurations B, C, D, E, and F, respectively. These thrust coefficients remained nearly constant over a range of nozzle pressure ratios from 2 to 15. For example, the thrust coefficient for configuration B, which generally had the highest thrust coefficient above a pressure ratio of 2.5, remained above 0.95 at nozzle pressure ratios from 2.5 to 12.

The ratio of the outer-shell exit area to the throat area (that is, the ratio of the projected area of the downstream end of the outer shell to the nozzle throat area  $A_g/A_t$  of an extended-plug nozzle) corresponds, in a sense, to the physical expansion ratio of a convergent-divergent nozzle, and its effect on extended-plug-nozzle performance is similar to the effect of expansion ratio on convergent-divergent-nozzle performance. For example, the peak thrust coefficient appears to occur at higher nozzle pressure ratios as the ratio of outer-shell exit area to throat area increases for each configuration in figure 7. Increasing the ratio of outer-shell exit area to throat area also increased the drop in thrust coefficient at the low nozzle pressure ratios; however, the decrease in thrust coefficient was not nearly as severe as the loss in thrust coefficient due to overexpansion in convergent-divergent nozzles with peak thrust coefficients at comparable nozzle pressure ratios. This drop in thrust coefficient at the low nozzle pressure ratios is not necessarily an inherent characteristic of the extended-plug nozzle, as will be explained in a subsequent part of this report.

Configurations B, C, D, and E had some internal divergence due to the geometry of these configurations (see fig. 5(a)). Part of the decrease in thrust coefficient at the low nozzle pressure ratios was caused by overexpansion which resulted from the internal divergent section.

Performance of simulated iris-type extended-plug nozzle. - The foregoing discussion was concerned with nozzle throat-area variation by translation of the outer shell along the plug. Throat area can also be varied by an iris (variable exit diameter) outer shell. The variation of thrust coefficient with nozzle pressure ratio for a simulated iris-type nozzle is shown in figure 8 for three throat areas (configurations B, G, and H). Peak thrust coefficients for configurations B, G, and H were 0.96, 0.96, and 0.98, respectively. Configurations B and H had some internal divergence due to the geometry of the nozzle, with configuration H having an internal expansion ratio of 1.39. Although the thrust coefficient appeared to have been increased by the internal divergence of the nozzle (configuration H), the decrease in thrust coefficient due to overexpansion at the low nozzle pressure ratios was increased. With configuration G, a thrust coefficient above 0.95 was obtained up to a nozzle pressure ratio of 5.5, but underexpansion losses at higher nozzle pressure ratios were encountered because of the low ratio of outer-shell exit area to throat area.

Sensitivity to throat-area variation. - A comparison showing the effect of nozzle throat-area variation on the performance of both types of extended-plug nozzles, a convergent-divergent nozzle, and a convergent nozzle is shown in figure 9 for nozzle pressure ratios of 3 and 10. The extended-plug nozzles were composed of configurations A to F for the translatable-outer-shell-type nozzle and configurations B, G, and H for the simulated iris-type nozzle. The data for the convergent nozzle were taken from the performance of the simple conical convergent nozzle reported in reference 1. It was assumed for the convergent nozzle that the nozzle throat-area variation can be obtained by the use of either an iris or clamshell nozzle and that the thrust coefficient remains constant over a wide range of throat-area variation at each nozzle pressure ratio. Data from reference 4 were used as a basis for the variable-throat convergent-divergent nozzle, and data from references 1 and 2 were used to extrapolate the nozzle performance to the desired throat-area variation. The variable-throat convergent-divergent nozzle had a fixed exit area and a variation of relative throat area  $A_r$  from 1 to 1.735 which resulted in an expansion-ratio variation from 1.125 to 1.95.

At a nozzle pressure ratio of 3 (fig. 9(a)), the thrust coefficients of the extended-plug nozzle with the translatable outer shell and the variable-throat convergent-divergent nozzle were practically equal above a relative throat area of 1.35. The thrust coefficient of the iris-type extended-plug nozzle was less than the thrust coefficients of these nozzles above a relative throat area of 1.5. However, below a relative throat area of 1.35, the thrust coefficient of the variable-throat convergent-divergent nozzle decreased rapidly because of severe overexpansion losses, whereas both extended-plug nozzles maintained relatively high thrust coefficients. The decreases in thrust coefficient of the extended-plug nozzles were not severe at the low relative

throat areas, and the thrust coefficients of both of these nozzles remained above 0.93 down to a relative throat area of 1.0. For this low nozzle pressure ratio, the convergent nozzle had a thrust coefficient of 0.975 over the full range of relative throat areas.

At a nozzle pressure ratio of 10 (fig. 9(b)), the extended-plug nozzles had thrust coefficients which were as much as 2 percentage points lower than those of the variable-throat convergent-divergent nozzle at relative throat areas below 1.5. The thrust coefficients of both extended-plug nozzles were higher than the thrust coefficient of the variable-throat convergent-divergent nozzle at higher relative throat areas, because the underexpansion of the extended-plug nozzles was less severe than that of the variable throat convergent-divergent nozzle. Severe underexpansion decreased the thrust coefficient of the convergent nozzle to a value of 0.915 at a nozzle pressure ratio of 10 for all relative throat areas.

For a relative throat area of 2, the translatable-outer-shell extended-plug nozzle approached a convergent nozzle (configuration A) and the thrust coefficient decreased as a result of underexpansion losses at a nozzle pressure ratio of 10; the thrust coefficient of the iris-type nozzle remained high because of an increasing ratio of outer-shell exit area to throat area and internal divergence.

#### Effect of Plug Shape

Some of the effects of throat-area variation on thrust coefficient for several nozzles which had a common plug were discussed in the preceding paragraphs. In order to show briefly the effect of extreme variation in plug shape on nozzle thrust coefficient and to determine an end point of plug design, configurations I and J (see table I) were investigated and the resultant thrust coefficients are shown in figure 10 over a range of nozzle pressure ratios. The downstream face of the blunt plug of configuration J was located in the plane of the outer-shell exit. Configurations I and J had the same ratio of outer-shell exit area to throat area, but the thrust coefficients of configuration J were generally about 2 to 4 percent lower than those of configuration I. The generally poorer performance of the blunt plug as compared with the conical plug was attributed to the expansion of the gas stream around the corner of the plug which caused the pressure on the downstream surface of the plug to be lower or as low as the ambient pressure at the low nozzle pressure ratios. The thrust gains over a simple convergent nozzle that were observed above a nozzle pressure ratio of 8 for configuration J indicate a higher than ambient pressure acting on the downstream plug surface. Even though configuration I had no internal divergence, the thrust coefficient was at least as high as for any of the configurations shown in figure 7; this indicates that internal divergence is not essential to obtaining high thrust coefficients with this type of nozzle.



### Plug Pressure Distribution

Plug-wall pressures are plotted in figure 11 against plug projected area at the pressure-measuring station for configurations A to I at various nozzle pressure ratios. An abrupt decrease in wall pressure occurred immediately downstream of the plug corner in each configuration as a result of the Prandtl-Meyer expansion of the flow around the corner. This decrease represents a loss in jet thrust since the pressure drop reduces a forward-acting pressure force on a large percentage of the plug area to below that which could be obtained in an ideal expansion.

Overexpansion resulting from an internal divergent section is also evident from these pressure curves. It was pointed out in connection with figure 10 (configuration I) that an internal divergent section is not essential to obtaining high thrust coefficients at high nozzle pressure ratios. An extended-plug nozzle having a faired plug (no sharp corners) with turning of the flow taking place in the subsonic region and having no internal divergent section would be expected to have a nearly flat thrust coefficient characteristic. Therefore, the losses in thrust coefficient at the low nozzle pressure ratios displayed by the configurations in this report were not necessarily an inherent characteristic of the extended-plug nozzle.

### Air-Flow Parameter

The corrected air-flow parameter for each configuration is plotted against nozzle pressure ratio in figure 12. The theoretical value of the air-flow parameter (0.344 lb/sec/sq in.) for critical flow is shown by a dashed line. The ratio of the experimental air-flow parameter to the theoretical value gives flow coefficients for these configurations ranging from 0.95 to 0.997 for critical flow. Some of the configurations did not unchoke until very low nozzle pressure ratios were reached, because an internal divergent section kept them overexpanded.

### SUMMARY OF RESULTS

In an experimental investigation of large-scale jet nozzles, a preliminary evaluation of the internal performance characteristics of several variable-throat extended-plug-type nozzles was made over a range of nozzle pressure ratios from 1.5 to 15 with nozzle throat-area variations as great as 2:1, and the following results were obtained:

1. The thrust coefficients of an extended-plug nozzle remained relatively constant over a wide range of nozzle pressure ratios. A thrust coefficient of 0.95, equal to that of a fixed-geometry convergent-divergent nozzle, was obtained for a typical extended-plug nozzle at a

nozzle pressure ratio of 16. At a nozzle pressure ratio of 2, the thrust coefficient of the extended-plug nozzle was reduced to 0.935 as compared with 0.82 for the convergent-divergent nozzle. This difference in thrust coefficient resulted from overexpansion losses, which were much smaller for the extended-plug nozzle than for the convergent-divergent nozzle.

2. The thrust coefficient of the variable-throat extended-plug nozzle (which averaged about 0.95) was relatively insensitive to throat-area variations. At a nozzle pressure ratio of 3, a comparison of the variable-throat extended-plug nozzle with a variable-throat convergent-divergent nozzle showed the performance to be comparable above relative throat areas (ratio of nozzle throat area to minimum nozzle throat area) of 1.5. For relative throat areas from 1 to 1.5, the thrust coefficients for the extended-plug nozzles were up to 9 percentage points higher than the convergent-divergent nozzle. This difference in thrust coefficient at the lower relative throat areas occurred because the overexpansion losses of the convergent-divergent nozzle were greater. At a nozzle pressure ratio of 10, the thrust coefficients for the extended-plug nozzles were as much as 2 percentage points lower than those of the convergent-divergent nozzle for a relative throat area from 1 to 1.5. Above a relative throat area of 1.5, the thrust coefficients for the extended-plug nozzles were up to 4 percentage points higher than for the convergent-divergent nozzle. The thrust coefficient of the convergent-divergent nozzle dropped below that of the extended-plug nozzle at the higher relative throat areas because of greater underexpansion. For choked flow, the extended-plug nozzles had flow coefficients varying from 0.95 to 0.997.

3. The ratio of outer-shell exit area to throat area was found to have an effect on the nozzle performance. As this area ratio was increased, the peak thrust coefficients occurred at higher nozzle pressure ratios and were accompanied by greater decreases in thrust coefficient at the low nozzle pressure ratios. The decrease in thrust coefficient at low nozzle pressure ratios is not necessarily an inherent characteristic of the extended-plug nozzle, and it is believed that this drop in thrust coefficient can be nearly eliminated by proper nozzle design.

Lewis Flight Propulsion Laboratory  
National Advisory Committee for Aeronautics  
Cleveland, Ohio, November 9, 1953

## APPENDIX A - SYMBOLS

The following symbols are used in this report:

A	outside area, sq ft
A'	inside area, sq ft
A <sub>f</sub>	flow area, sq ft
A <sub>l</sub>	pipe area under labyrinth seal, sq ft
A <sub>p</sub>	plug projected area, sq ft
A <sub>r</sub>	ratio of nozzle throat area to minimum nozzle throat area
A <sub>s</sub>	exit area of outer shell, sq ft
A <sub>t</sub>	throat area, sq ft
C <sub>T</sub>	thrust coefficient
C <sub>x</sub>	thermal-expansion ratio, ratio of heated area to cold area
F	thrust, lb
F <sub>d</sub>	balanced-air-pressure-diaphragm reading, lb
g	acceleration due to gravity, 32.174 ft/sec <sup>2</sup>
l	length, in.
P	total pressure, lb/sq ft
p	static pressure, lb/sq ft
P <sub>bm</sub>	integrated static pressure acting on outside of bellmouth inlet to station 2, lb/sq ft
p <sub>d</sub>	integrated pressure acting on outside of diffuser, lb/sq ft
R	gas constant, 53.3 ft-lb/(lb)(°R) for air
T	total temperature, °R
V	velocity, ft/sec
W <sub>a</sub>	measured air flow, lb/sec

- $\delta$  ratio of total pressure at nozzle inlet to absolute pressure at  
NACA standard sea-level conditions
- $\gamma$  ratio of specific heats
- $\theta$  ratio of total temperature at nozzle inlet to absolute temperature  
at NACA standard sea-level conditions

## Subscripts:

- e nozzle exit
- i ideal
- j jet
- p plug
- t throat
- w plug surface or wall
- 0 exhaust or ambient
- 1 inlet
- 2 diffuser inlet
- 3 nozzle inlet

3071

CF-2 back

## APPENDIX B - METHODS OF CALCULATION

Air flow. - The nozzle air flow was calculated as

$$W_a = \frac{p_2 A_2' C_x}{\sqrt{RT_3}} \sqrt{\frac{\gamma-1}{\gamma} \left[ \left( \frac{p_2}{p_2'} \right)^{\frac{\gamma-1}{\gamma}} - 1 \right] \frac{p_2}{p_2'}}$$

with  $\gamma$  assumed to be 1.4. Values of the thermal expansion ratio  $C_x$  of the areas at the respective stations were obtained from the thermal-expansion coefficient for the material and the temperature of the material. The material temperature was assumed to be the same as the temperature of the air flowing through the respective station.

Thrust. - The jet thrust was defined as

$$F_j = \frac{W_{a,2}}{g} V_e + A_{f,e} (p_e - p_0) + \int_0^{A_{p,e}} p \, dA_p - p_e A_{p,e}$$

or as defined in the conventional manner

$$F_j = \frac{W_{a,2}}{g} \bar{V}_e + A_s (\bar{p}_e - p_0)$$

where  $\bar{V}_e$  and  $\bar{p}_e$  are effective values. The actual jet thrust was calculated by the equation

$$F_j = \frac{W_{a,2}}{g} V_1 + p_1 A_1' C_x + p_d (A_3 - A_2) C_x - p_{bm} (A_1' - A_2) C_x - p_0 A_3 C_x - F_d$$

where  $F_d$  was obtained from balanced-air-pressure-diaphragm measurements. The values of  $p_1$  and  $V_1$  were computed by use of one-dimensional flow relationships from the total and static pressures measured at station 2 and the total temperature measured at station 3. This method was checked and found accurate by actual preliminary pressure measurements at station 1.

The ideally available thrust, which was based on measured mass flow, was calculated as

$$F_i = W_a \sqrt{\frac{2R}{g} \frac{\gamma}{\gamma-1} T_3 \left[ 1 - \left( \frac{P_0}{P_3} \right)^{\frac{\gamma-1}{\gamma}} \right]}$$

Thrust coefficient. - The thrust coefficient is defined as the ratio of the actual to the ideal jet thrust

$$C_T = \frac{F_j}{F_i}$$

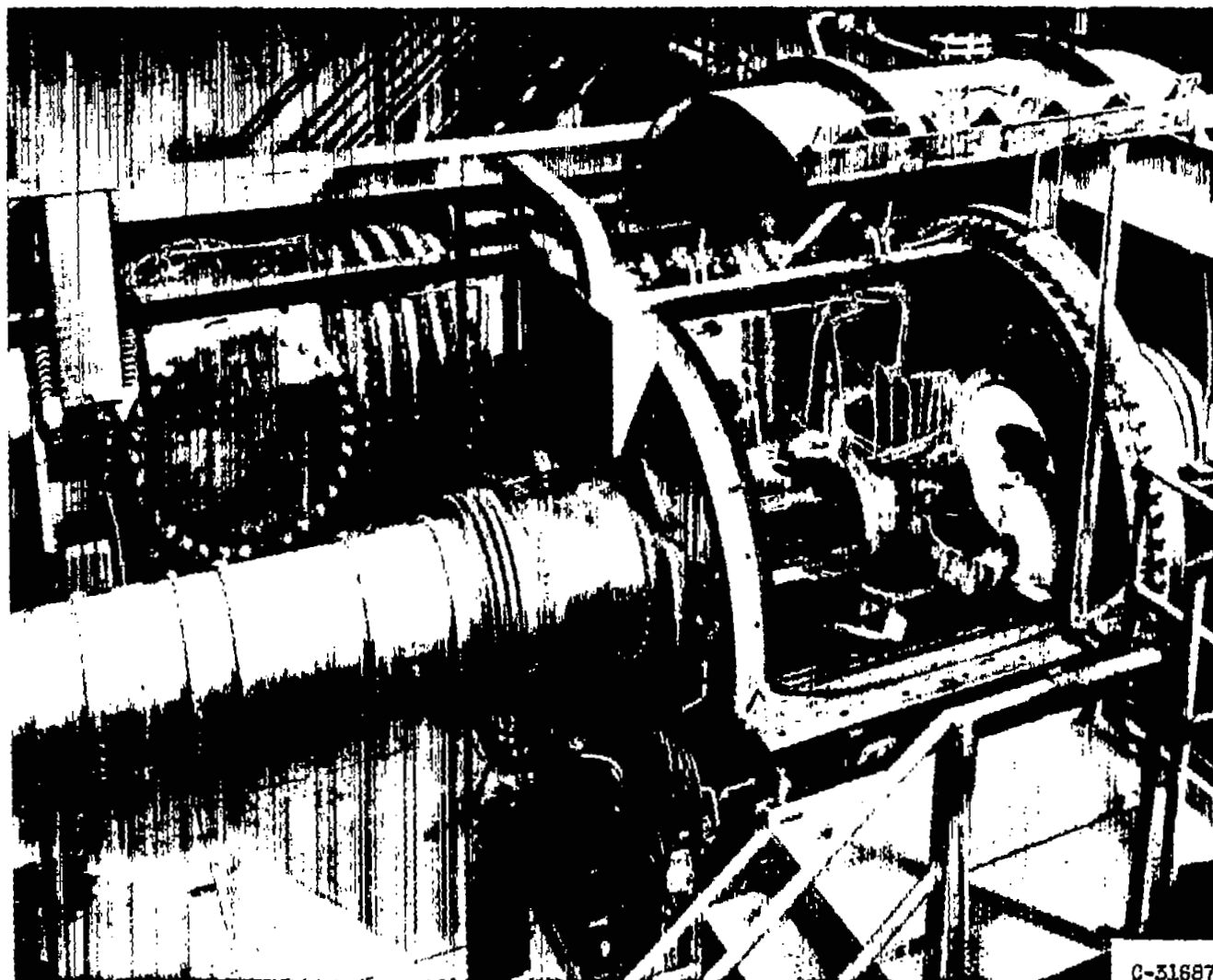
#### REFERENCES

1. Krull, H. George, and Steffen, Fred W.: Performance Characteristics of One Convergent and Three Convergent-Divergent Nozzles. NACA RM E52H12, 1952.
2. Schairer, G.: Performance Characteristics of Jet Nozzles. Doc. No. D-12054, Boeing Airplane Co., Seattle (Wash.), July 25, 1951.
3. Reshotko, Eli: Preliminary Investigation of a Perforated Axially Symmetric Nozzle for Varying Nozzle Pressure Ratios. NACA RM E52J27, 1953.
4. Krull, H. George, Steffen, Fred W., and Ciepluch, Carl C.: Internal Performance Characteristics of Variable-Throat-Plug- and Vaned-Type Convergent-Divergent Nozzles. NACA RM E53D09, 1953.

TABLE I. - NOZZLE CONFIGURATIONS

Configu- ration	Spool piece	Outer shell	Plug	Nozzle throat area, $A_t$ , sq in.	Nozzle- exit flow area, $A_{f,e}$ , sq in.	Internal expansion ratio, $A_{f,e}/A_t$	Outer-shell exit area
							Throat area $A_s/A_t$
	(a)	(a)	(a)				
A	1	1	1	86.59	86.59	1.0	1.0
B	2	1	1	67.86	78.14	1.15	1.28
C	3	1	1	59.43	69.68	1.17	1.46
D	4	1	1	53.06	61.25	1.15	1.63
E	5	1	1	47.91	52.38	1.09	1.81
F	-	1	1	43.23	43.23	1.0	1.98
G	2	2	1	48.16	48.16	1.0	1.18
H	2	3	1	89.37	124.28	1.39	1.48
I	-	3	1	89.37	89.37	1.0	1.48
J	-	3	2	89.37	89.37	1.0	1.48

<sup>a</sup>Numbers refer to parts shown in fig. 4.



C-31687

Figure 1. - Nozzle test chamber.



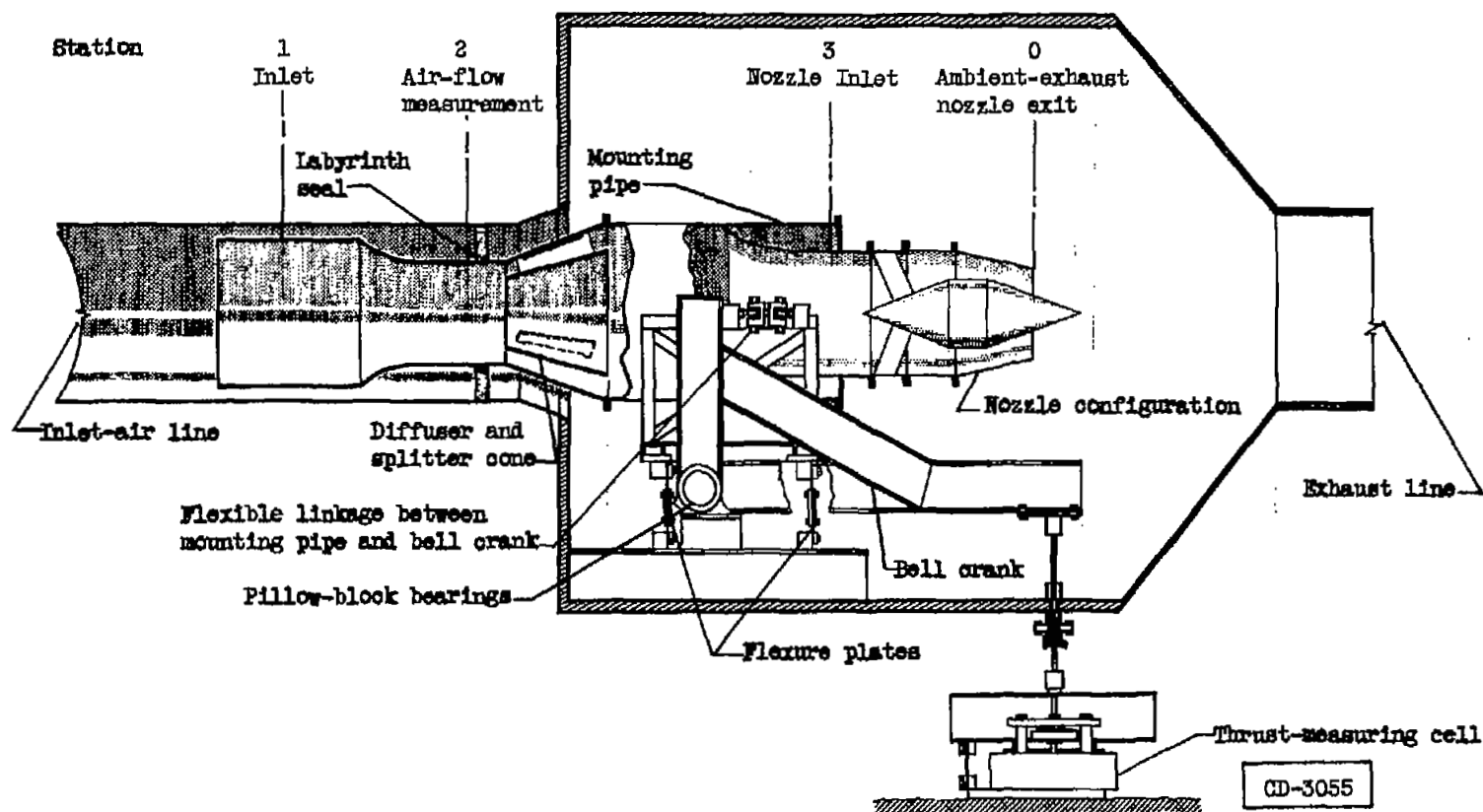
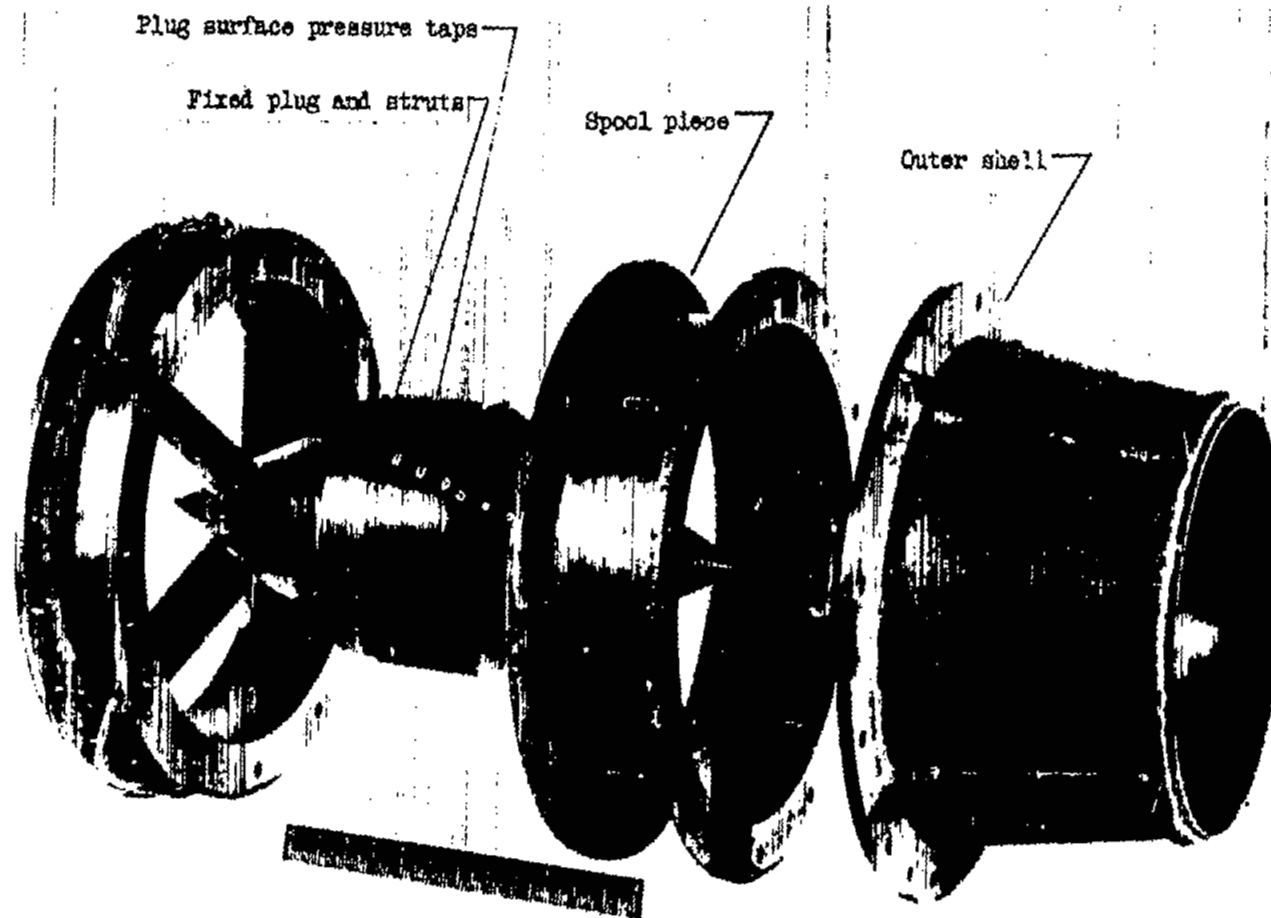
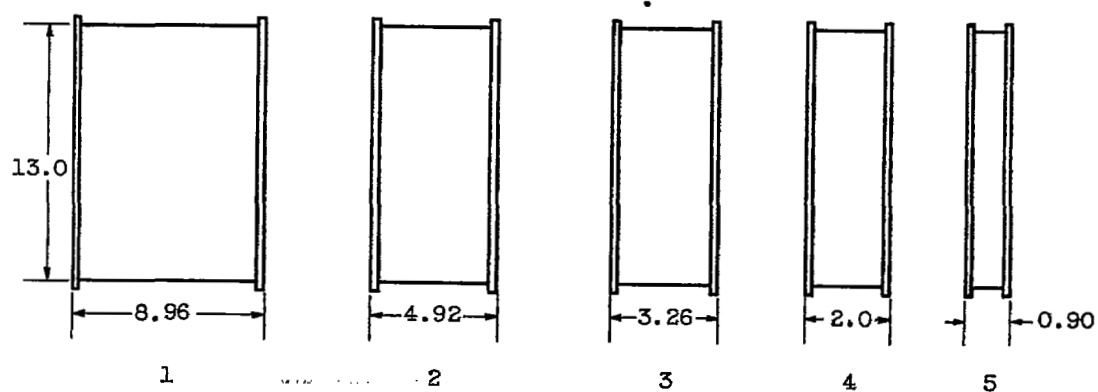


Figure 2. - Schematic drawing of nozzle in test chamber.

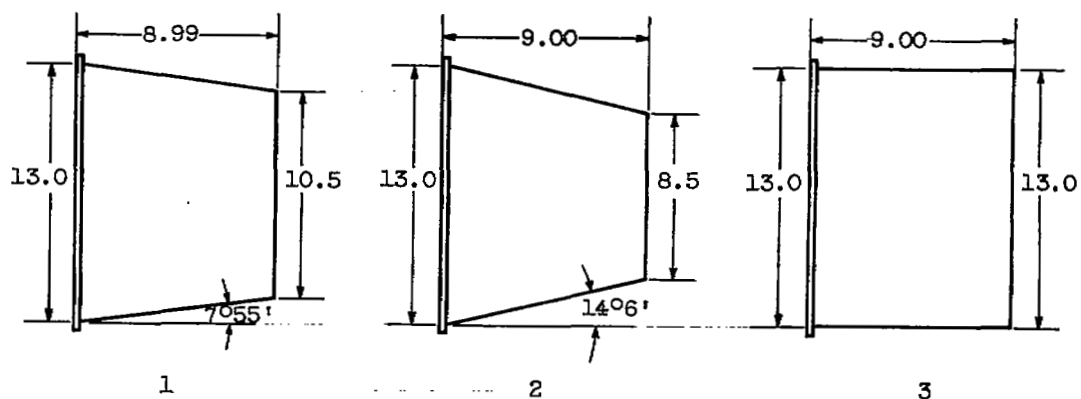


C-31107

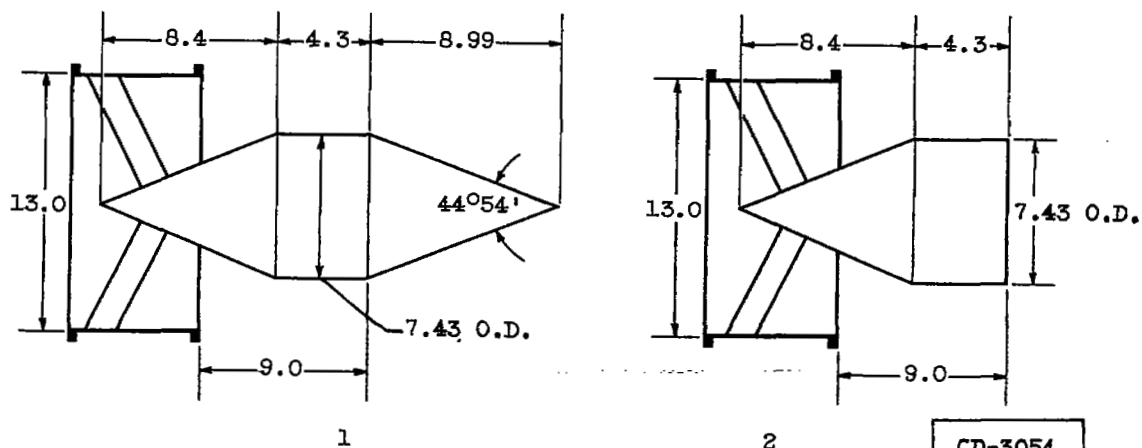
Figure 3. - Exploded view of nozzle assembly.



(a) Spool pieces.



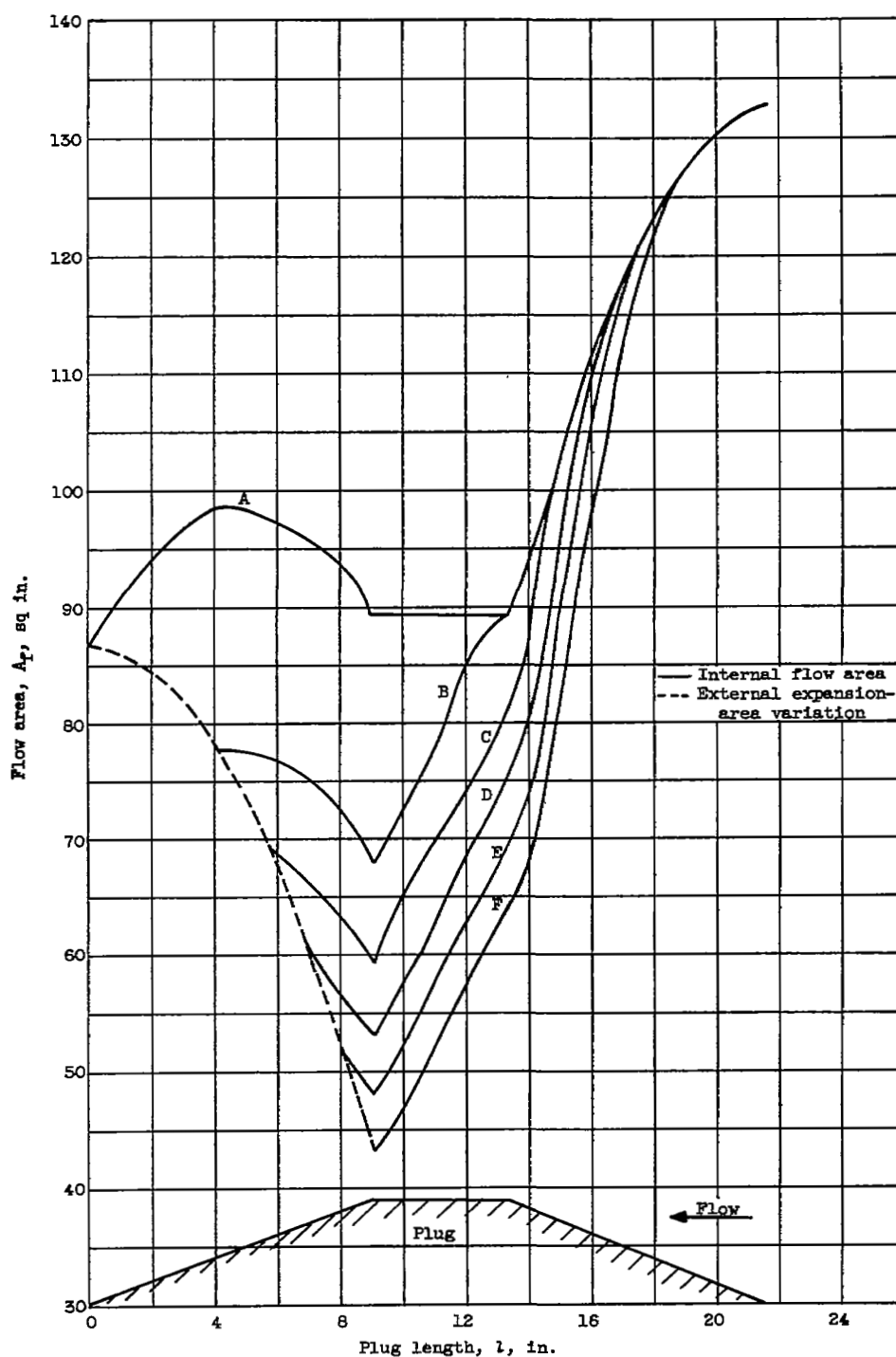
(b) Conical outer shells.



(c) Plugs.

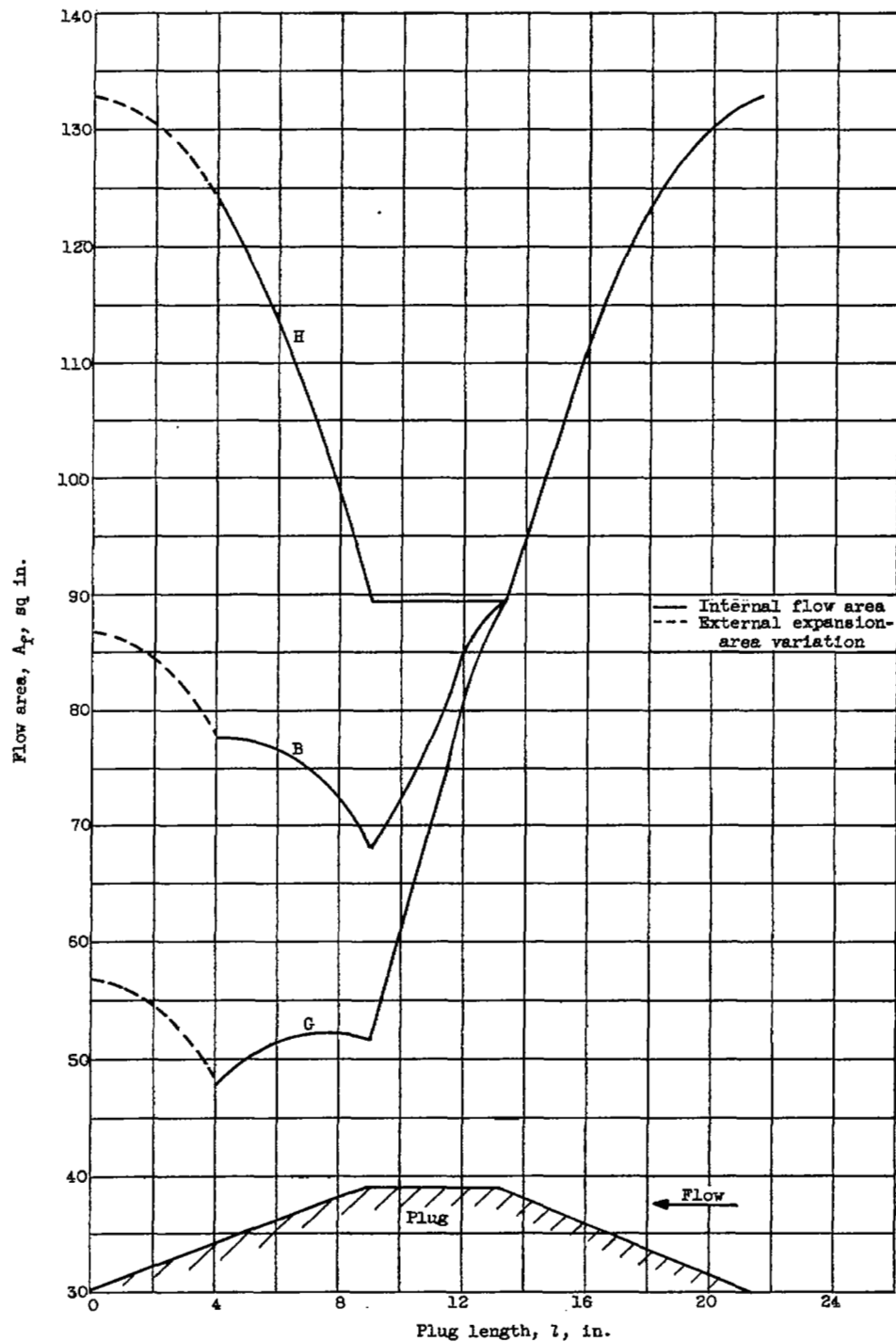
Figure 4. - Nozzle parts and dimensions. (All dimensions are in inches; all diameters are inside unless specified.)

CD-3054



(a) Translatable-outer-shell extended-plug nozzles, configurations A through F.

Figure 5. - Variation of nozzle flow area along plug.



(b) Iris-type extended-plug nozzle, configurations B, G, and H.

Figure 5. - Concluded. Variation of nozzle flow area along plug.

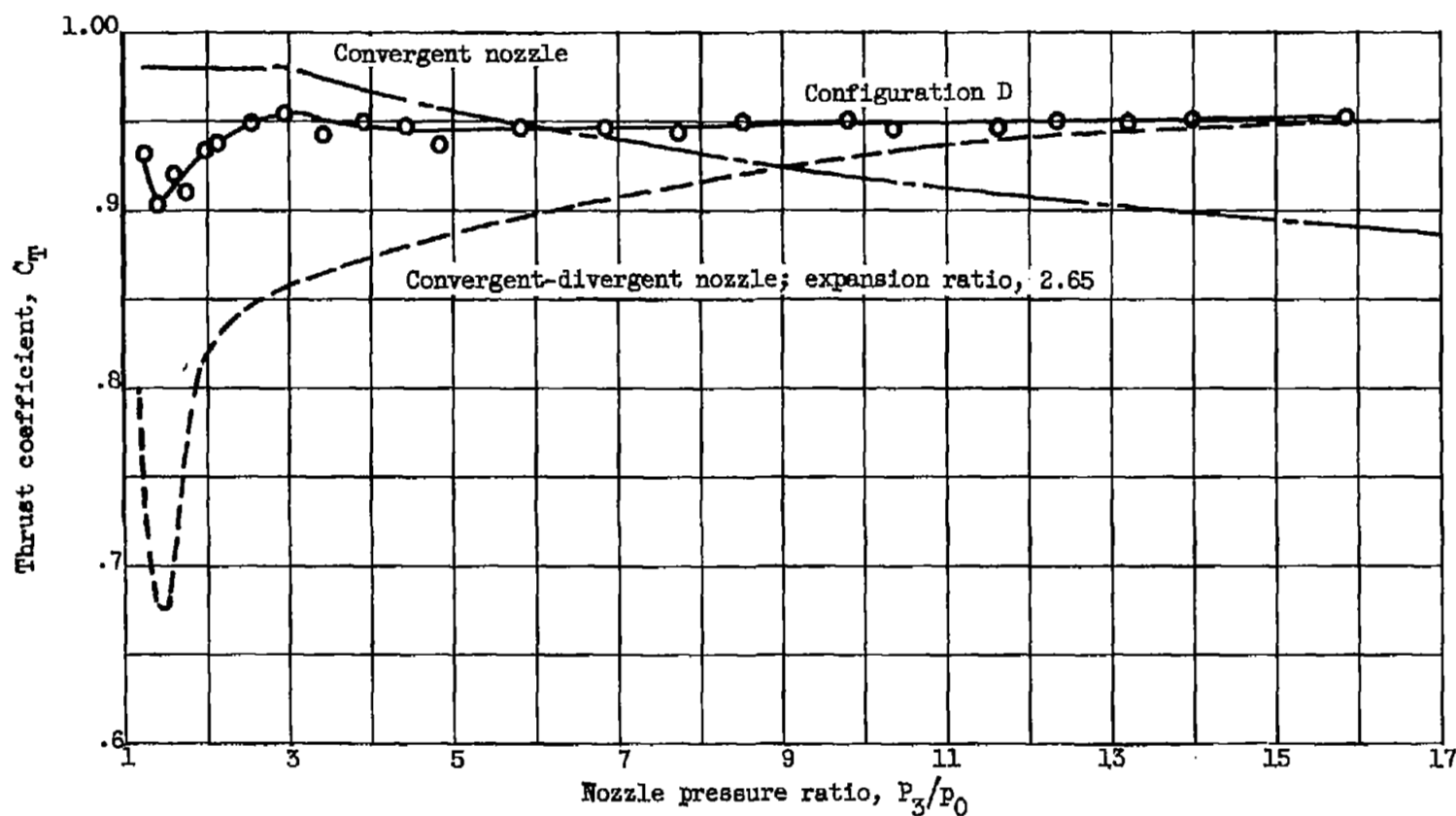


Figure 6. - Comparison of thrust coefficients of configuration D, convergent nozzle, and 2.65-expansion-ratio convergent-divergent nozzle over range of nozzle pressure ratios.

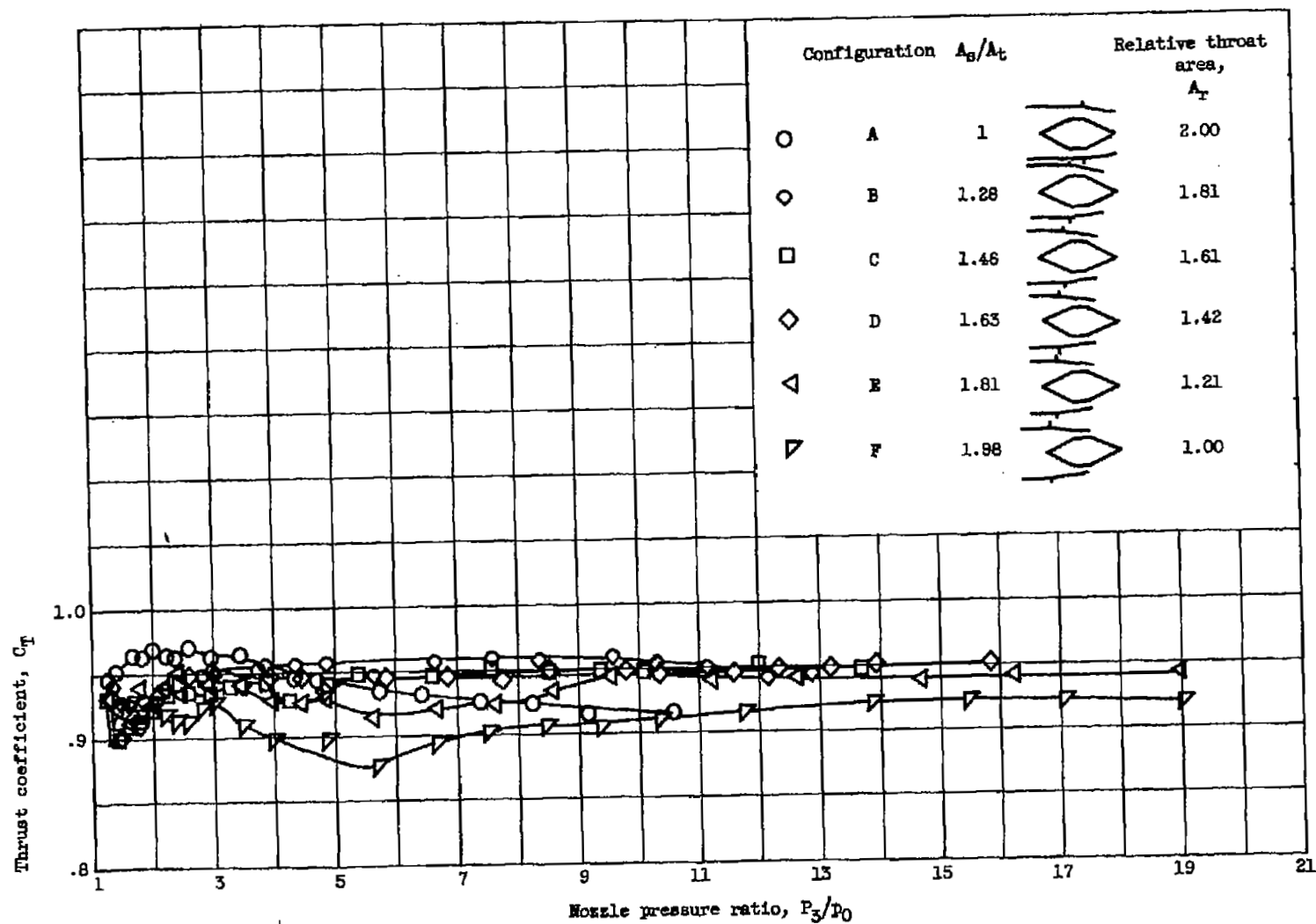


Figure 7. - Comparison of thrust coefficients over range of nozzle pressure ratios for configurations A through F.

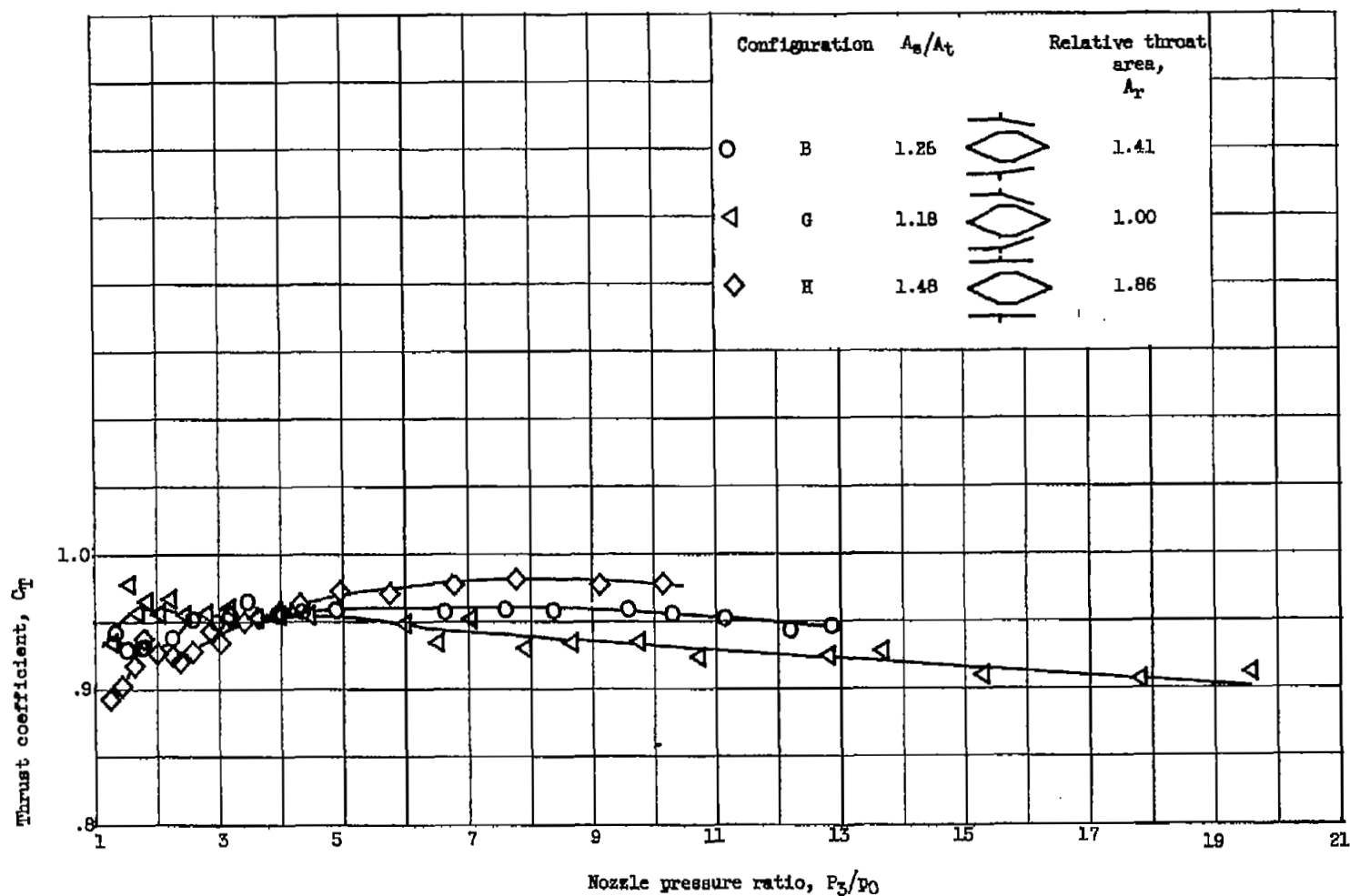


Figure 8. - Comparison of thrust coefficients over range of nozzle pressure ratios for configurations B, G, and H.



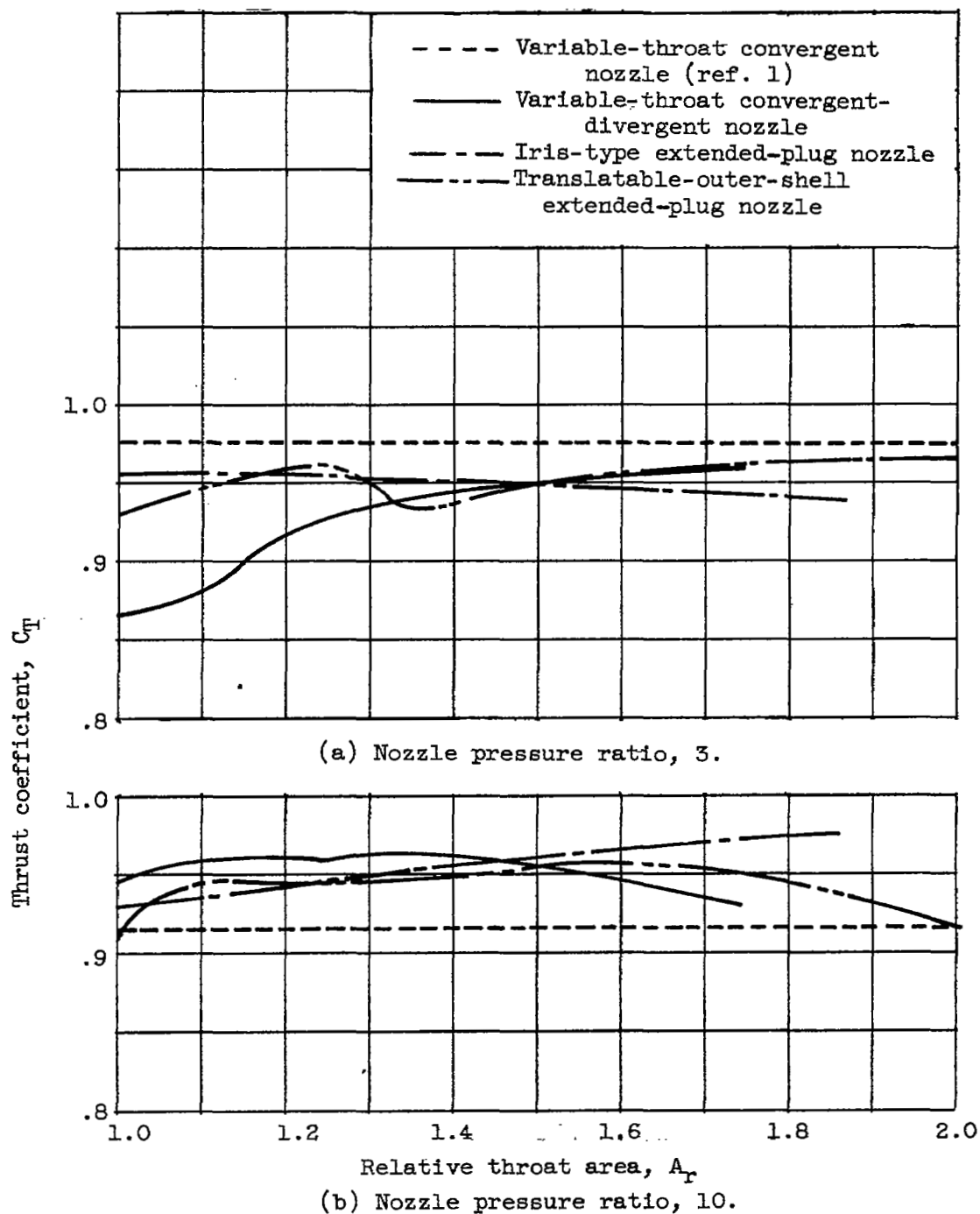
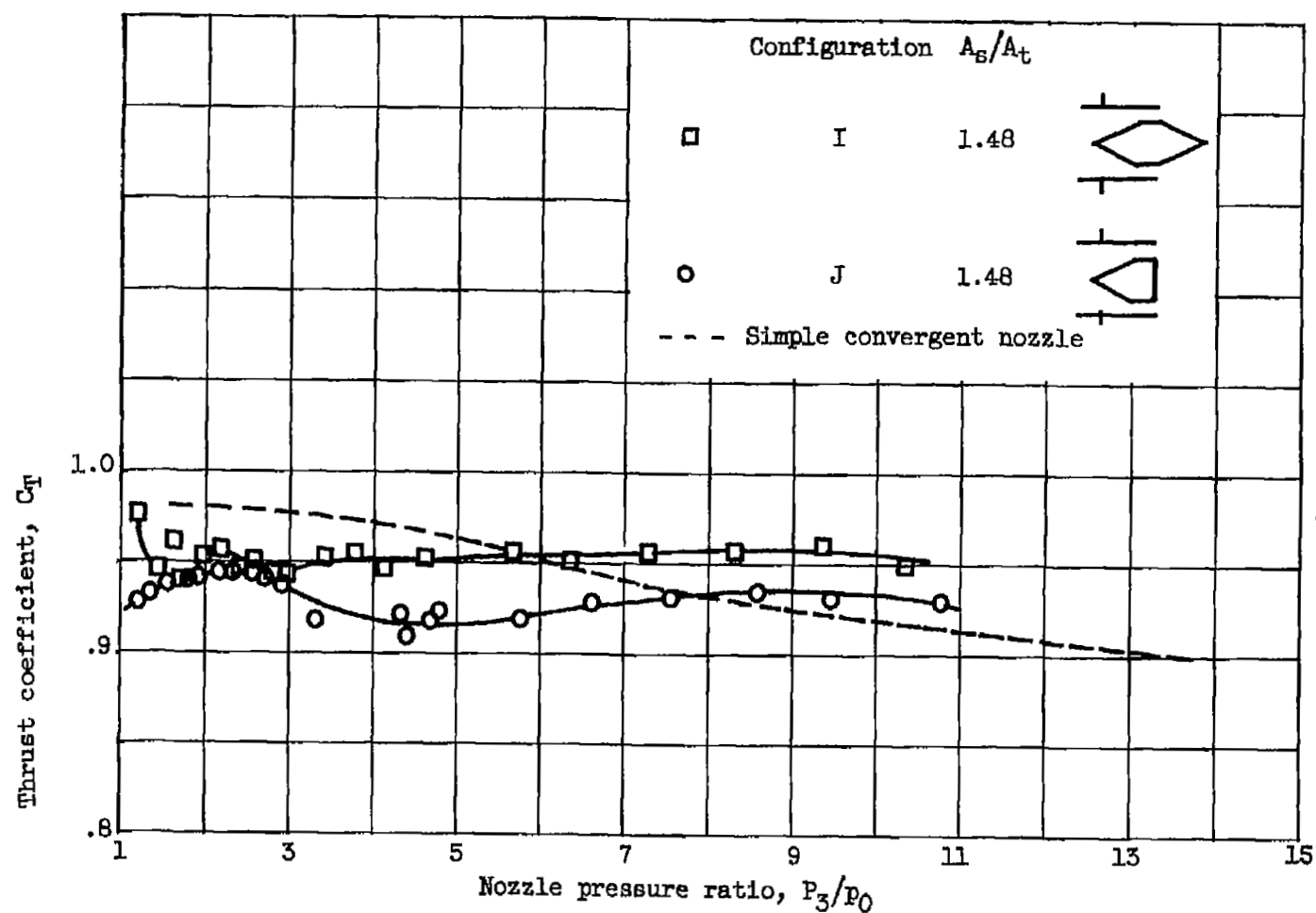


Figure 9. - Effect of throat-area variation on thrust coefficients of several nozzles at nozzle pressure ratios of 3 and 10.



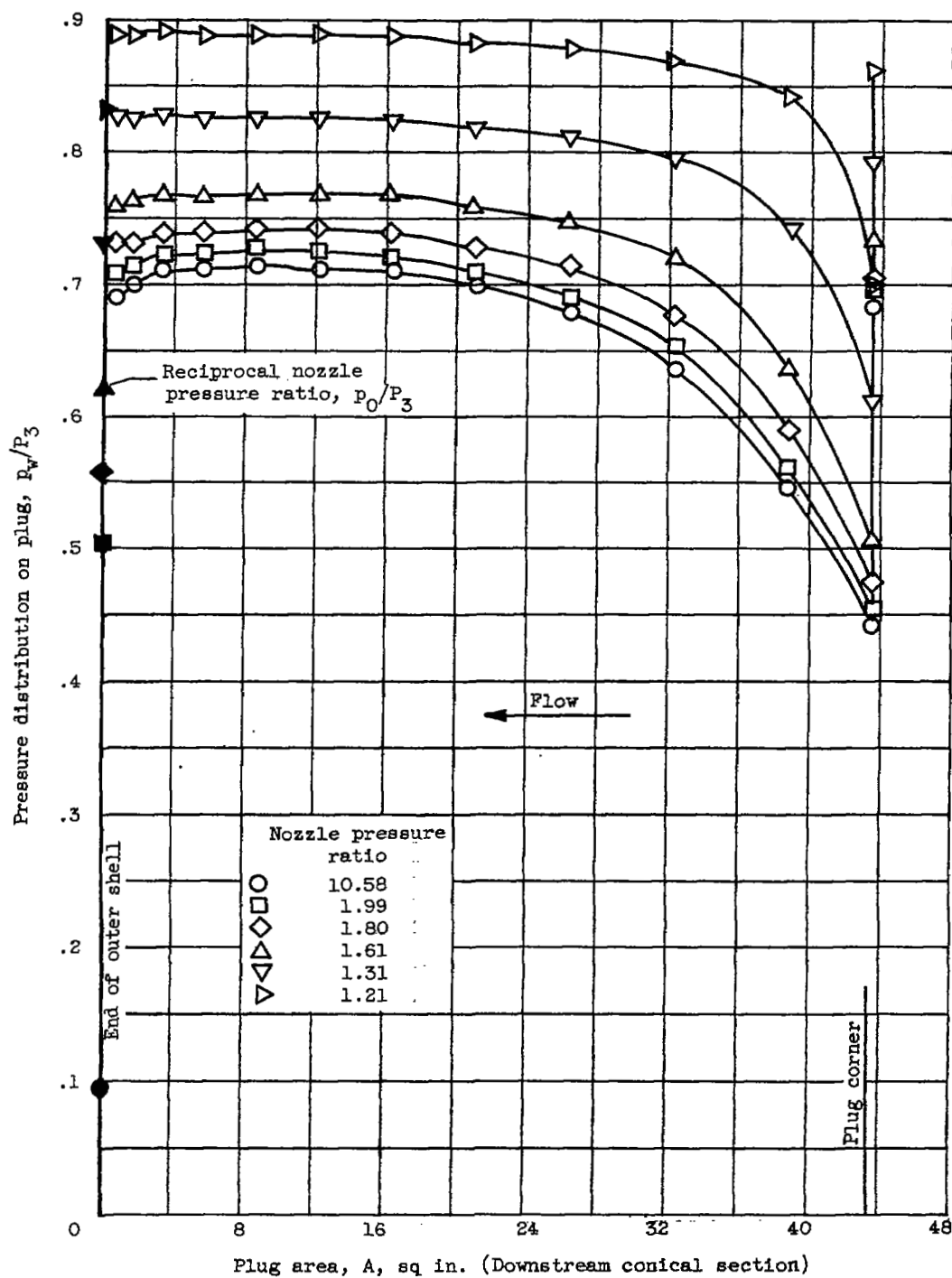
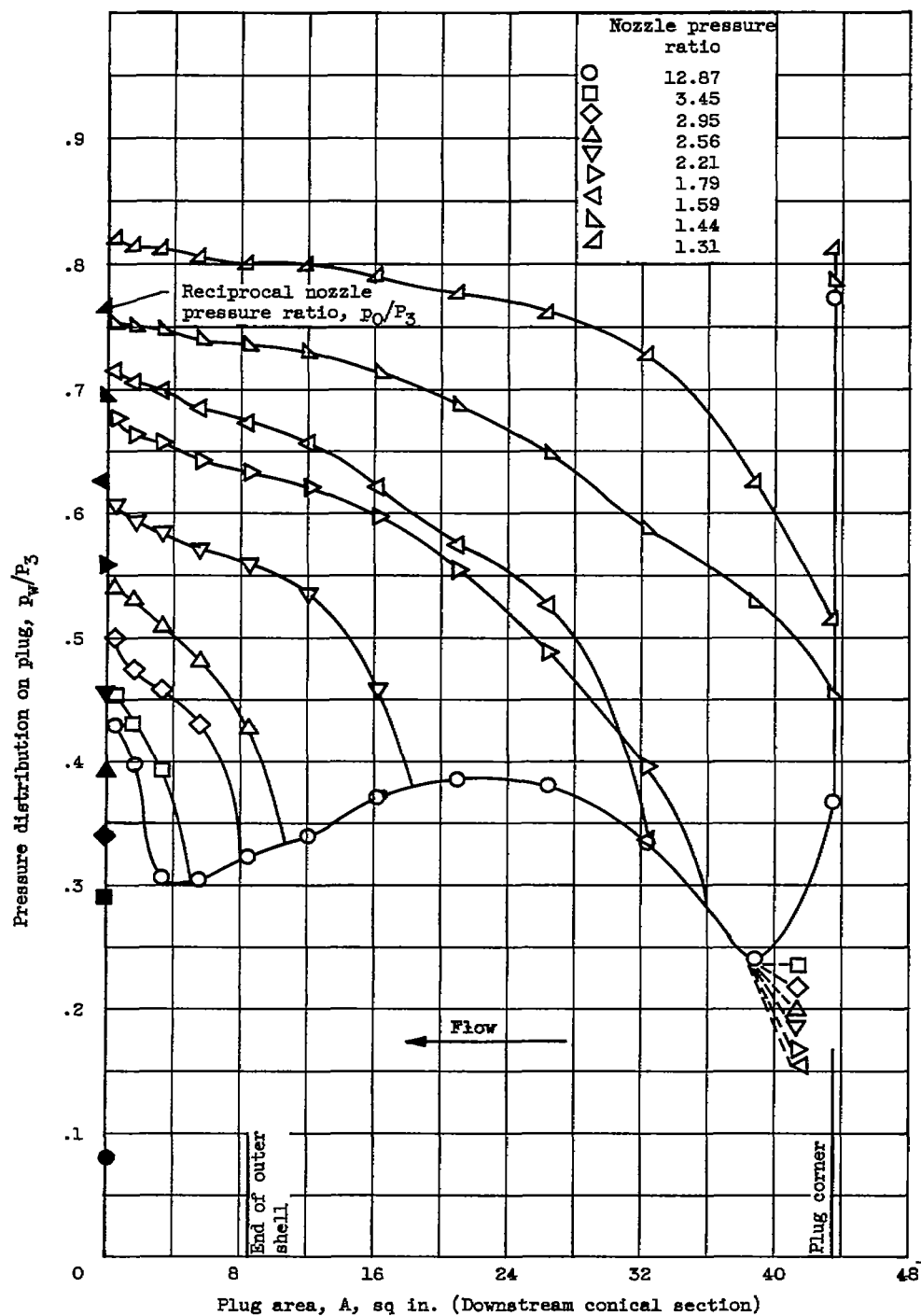


Figure 11. - Pressure distribution along plug surface at various nozzle pressure ratios.



(b) Configuration B.

Figure 11. - Continued. Pressure distribution along plug surface at various nozzle pressure ratios.

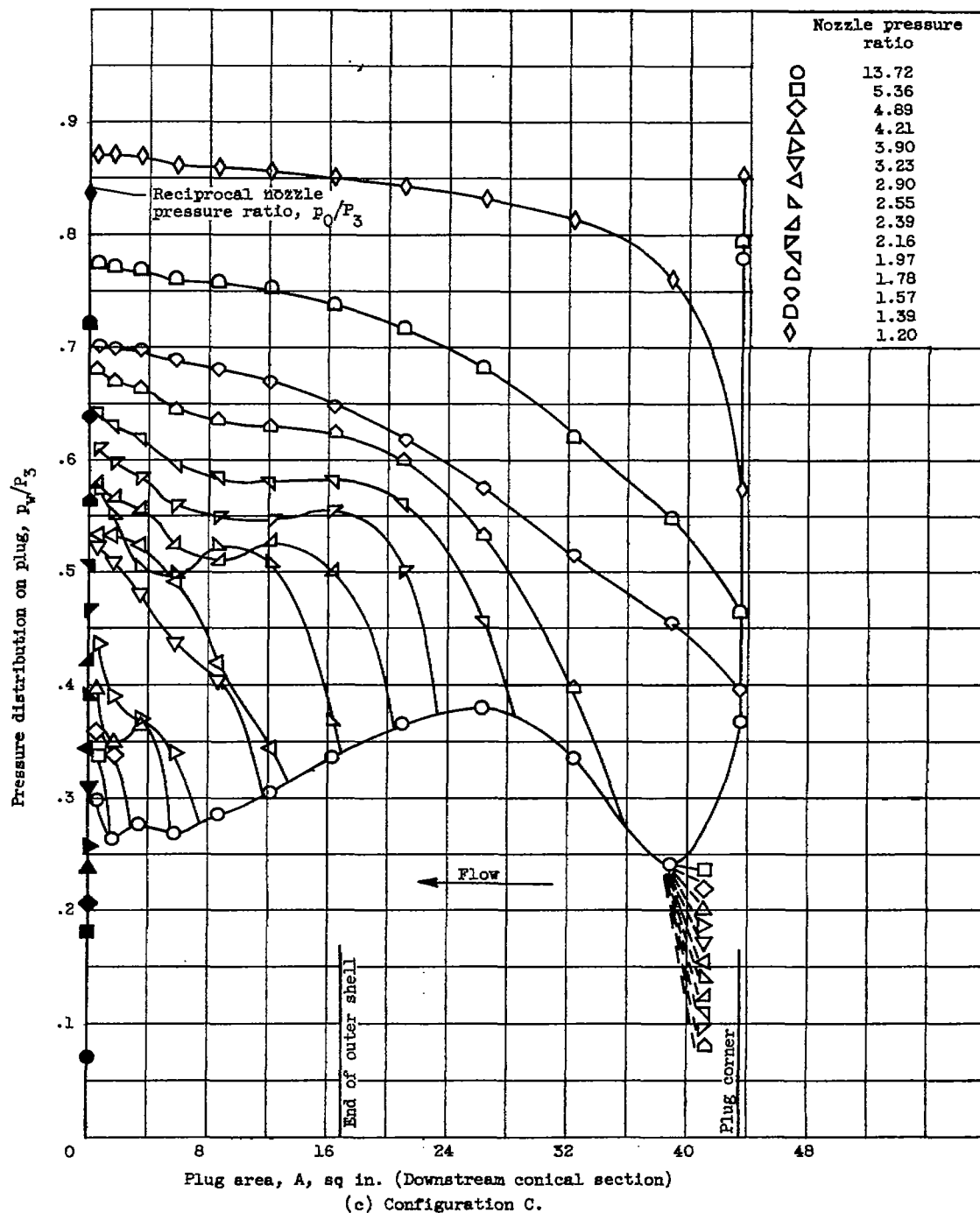
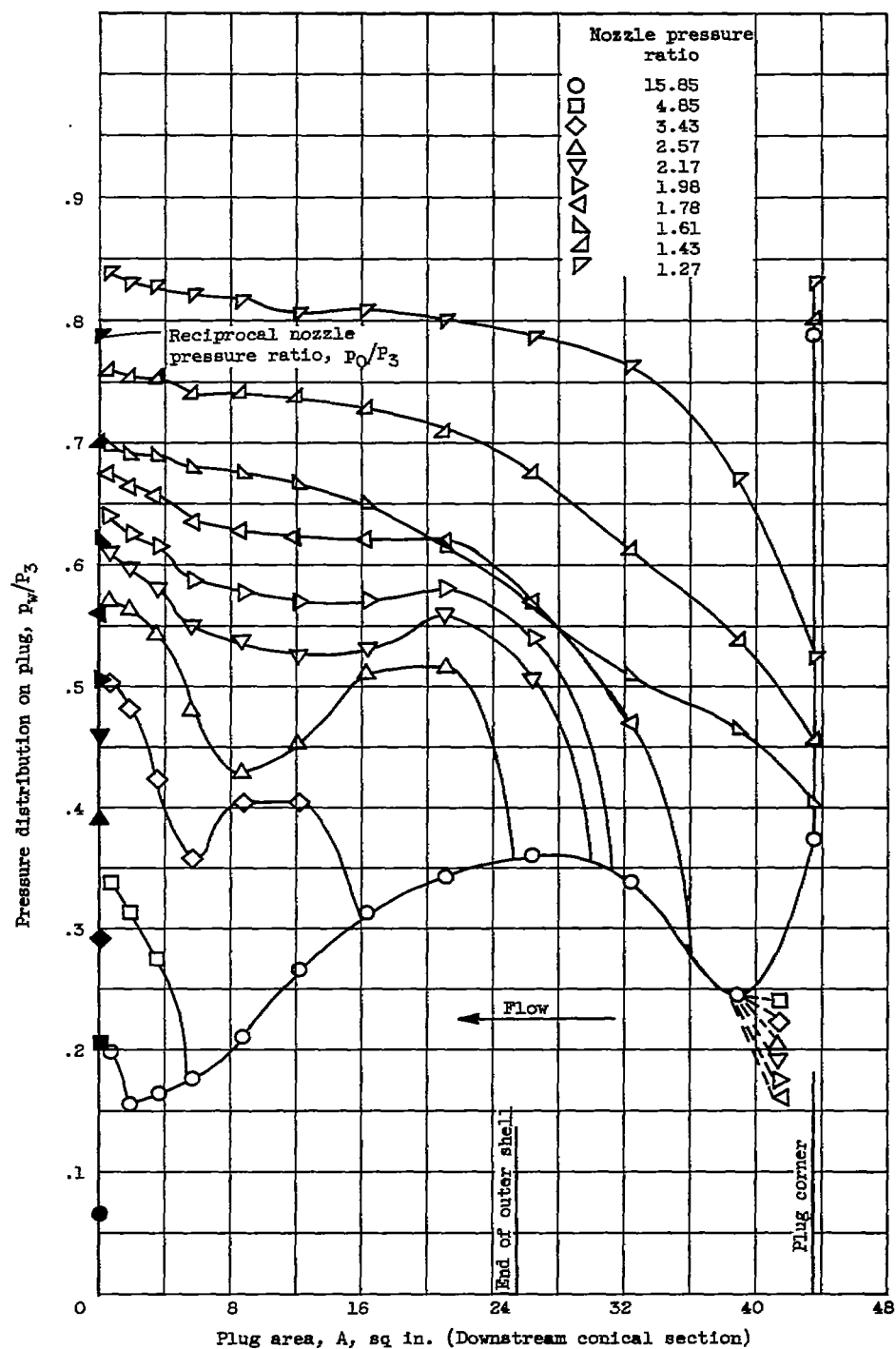
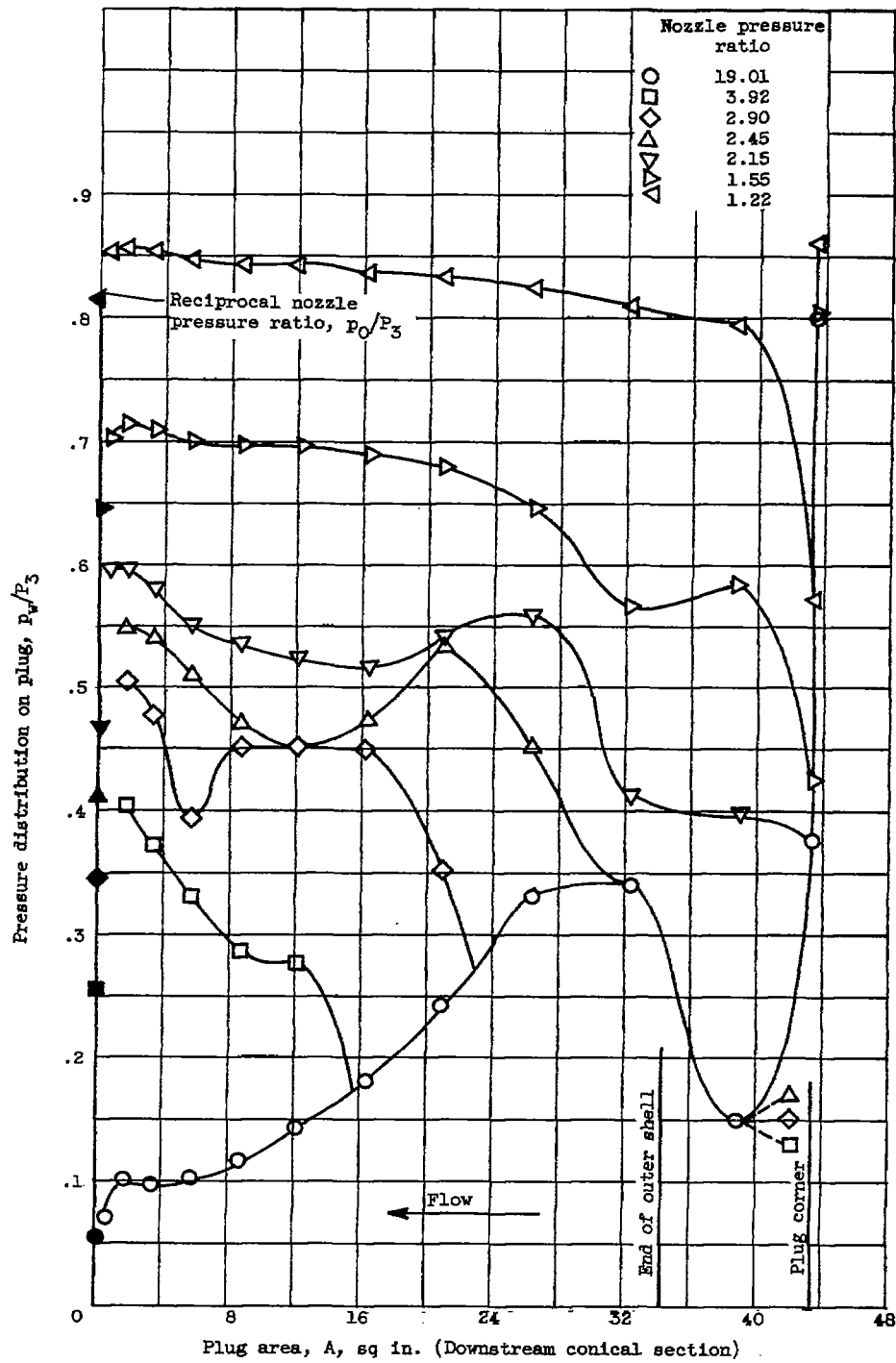


Figure 11. - Continued. Pressure distribution along plug surface at various nozzle pressure ratios.



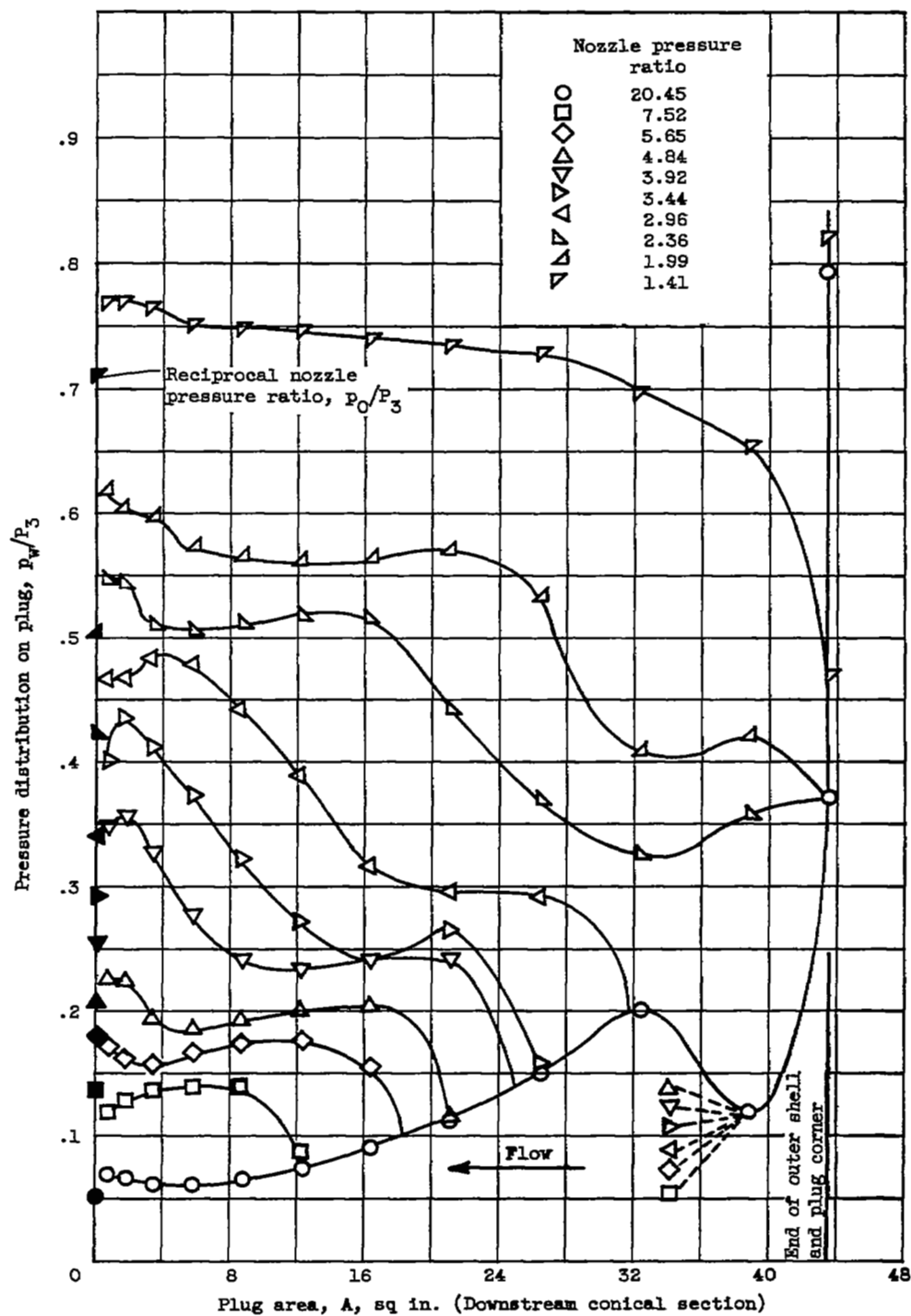
(a) Configuration D

Figure 11. - Continued. Pressure distribution along plug surface at various nozzle pressure ratios.



(e) Configuration E.

Figure 11. - Continued. Pressure distribution along plug surface at various nozzle pressure ratios.



(f) Configuration F.

Figure 11. - Continued. Pressure distribution along plug surface at various nozzle pressure ratios.



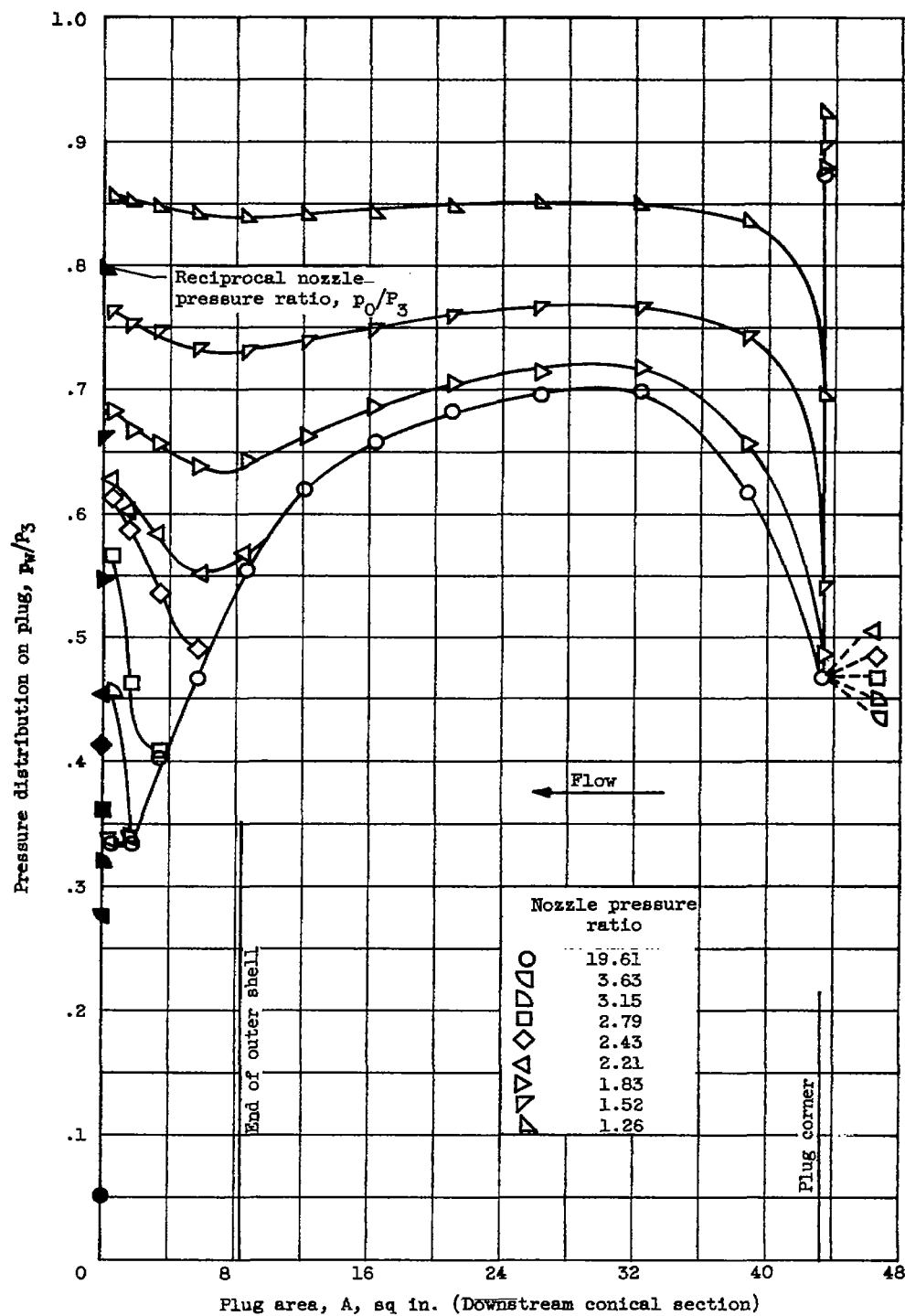


Figure 11. - Continued. Pressure distribution along plug surface at various nozzle pressure ratios.

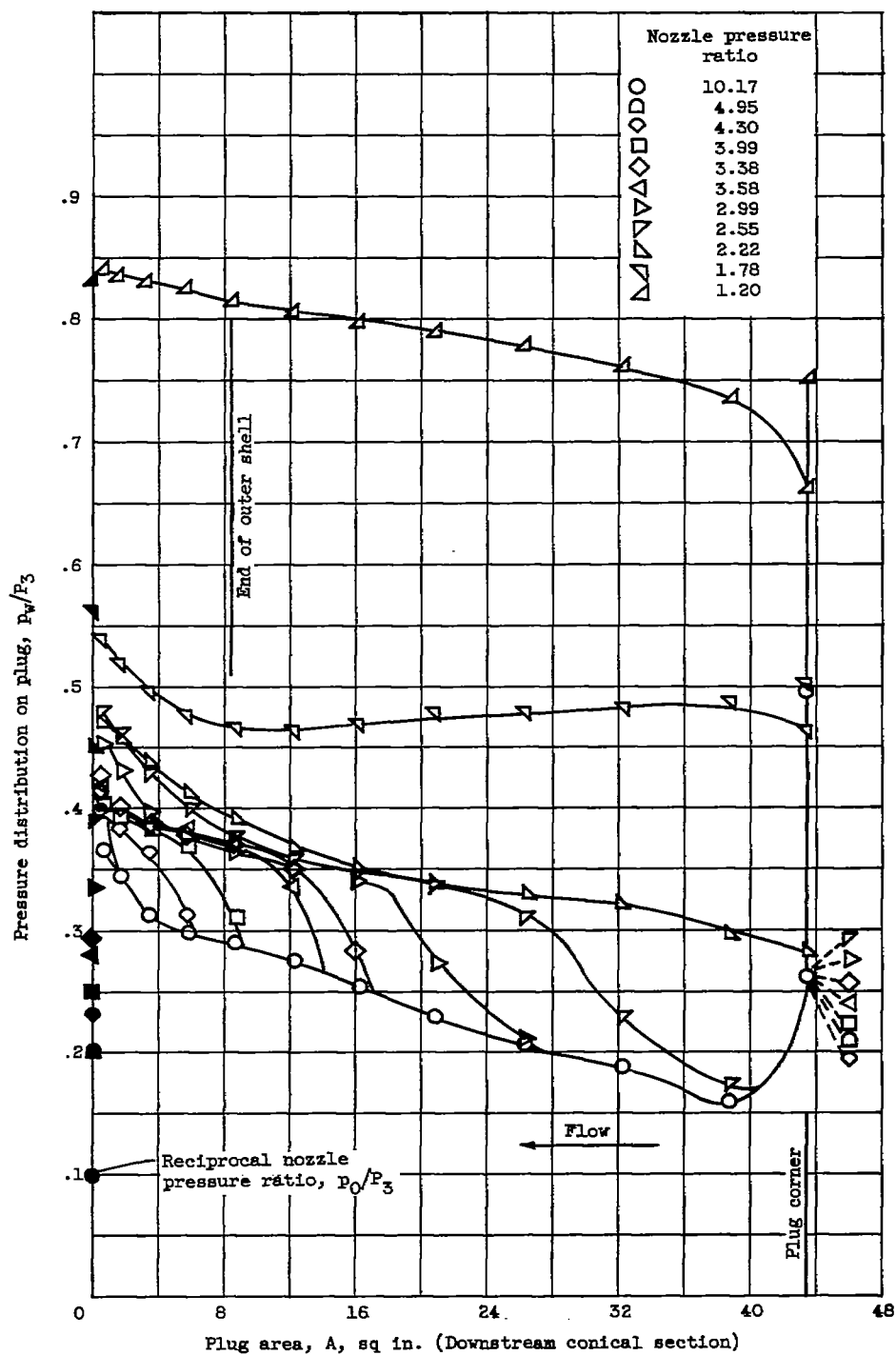
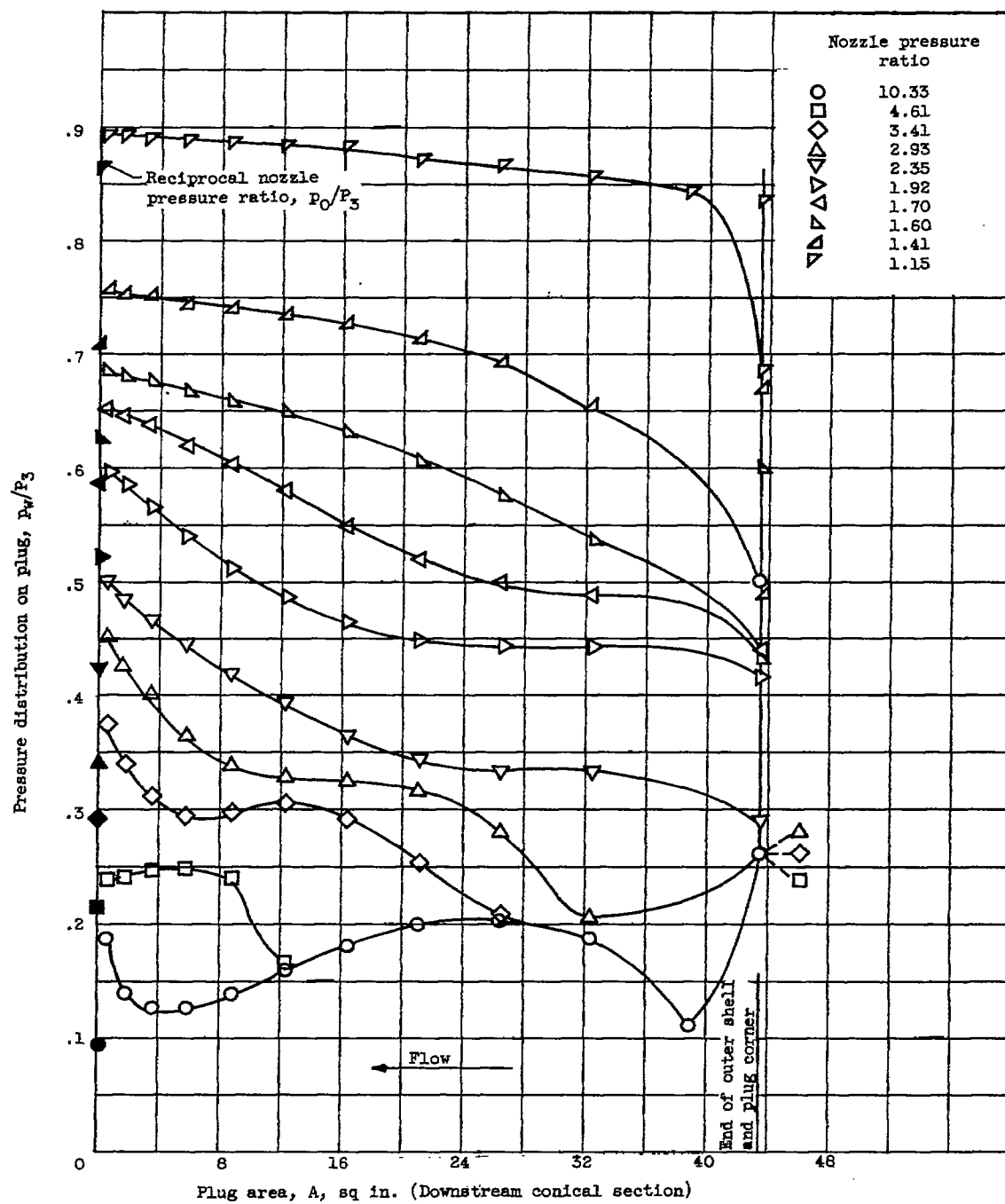


Figure 11. - Continued. Pressure distribution along plug surface at various nozzle pressure ratios.



(i) Configuration I.

Figure 11. - Concluded. Pressure distribution along plug surface at various nozzle pressure ratios.

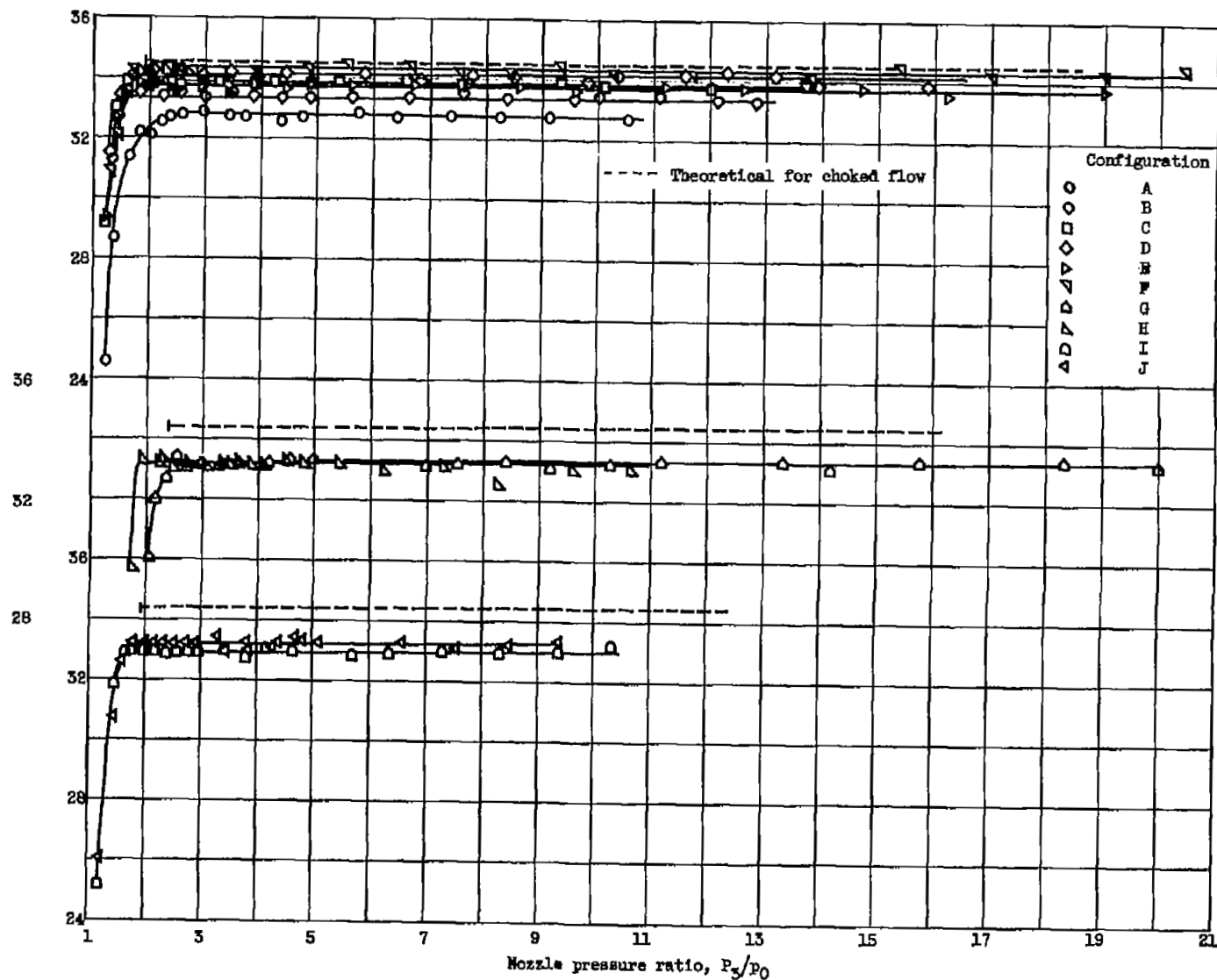
Corrected air-flow parameter,  $\frac{W_a/\beta}{A_{t,r}}$ , lb/sec/sq in.

Figure 12. - Variation of air-flow parameter with nozzle pressure ratio for configurations A through I.

NASA Technical Library



3 1176 01435 3040

